Fibers and Polymers 2004, Vol.5, No.2, 145-150

Effect of Metallocene-catalyzed Polyethylene on the Rheological and Mechanical Properties of Poly(phenylene sulfide)/Polyethylene Blends

Bo Sun Lee, Byoung Chul Chun*, and Yong-Chan Chung[1]

Department of Polymer Engineering, The University Suwon, Gyeonggi-do 445-743, Korea
[1]Department of Chemistry, The University of Suwon, Suwon, Gyeonggi-do 445-743, Korea
(Received October 23, 2003; Revised April 16, 2004; Accepted April 23, 2004)

Abstract: Blends of poly(phenylene sulfide) (PPS) and polyethylene, either linear low density polyethylene (LLDPE) or metallocene-catalyzed polyethylene (MPE), that were prepared by melt blending, were investigated. From the rheological properties as determined by capillary rheometry, the melt viscosity of both PPS/LLDPE and PPS/MPE blends was low when PE was in dispersed phase, but high melt viscosity was observed for both blends with PPS in dispersed phase. Significant differences depending on the composition were found in the mechanical properties such as percent elongation at break and notched Izod impact strength. In addition, dispersed phase morphology of the blends was analyzed by a scanning electron microscope (SEM), together with brief discussion about the difference between them.

Keywords: PPS, Blending, PE

Introduction

Poly(phenylene sulfide) (PPS), which was first discovered as by-product of Friedel-Crafts reaction in 1888 and commercialized by Philips Petroleum Co. in 1973, has been well known for exceptional dimensional stability, high strength, and fatigue and chemical resistance with relatively high T_g (80~90 °C) and T_m (280 °C). However, PPS is usually mixed with reinforcing glass fibers and applied in a composite material to make up its brittleness, low strain at break, and slow crystallization rate. So far, various blended PPSs such as PPS/thermoplastic polymer blend [1-3], PPS/glass-fiber-reinforced-composite [4-8], PPS/engineering plastic blend [9,10], and PPS/liquid crystalline polymer blend [11,12] have been reported to improve the mechanical strength of PPS, together with studies on crystallization mechanism and structure in which problems such as reproducible data and difficulty in data analysis still remain to be resolved. A common problem occurring in a PPS/polymer blend is weak interfacial bonding between two components, and the problem has been tried to be remedied by either dispersing derivatives such as polysulfone (PSF) or adding third component as interfacial bonding agent, where the second method fails because inherent properties of PPS can be damaged by the complexity of constituting components.

Meanwhile, a metallocene catalyst or so called a single-site catalyst introduced by Kaminsky and Sinn in 1980 significantly helped producing polymers with highly improved properties, drawing wide attention from scientific community. One of the outstanding performances of metallocene catalyst is the ability to control stereo-regularity of polymer structure and its property by adjustment of catalyst composition, resulting in narrow molecular weight distribution as well as homogeneous comonomer distribution in comparison with Ziegler-Natta catalyzed LLDPE [11]. In this investigation, PPS/LLDPE and PPS/MPE blends were compared in the points of rheological behavior, state of dispersion depending on PE used, and resultant mechanical property and morphology.

*Corresponding author: bcchun@mail.suwon.ac.kr

Experimental Section

Materials

PPS (Toprene, T-4, M_w = 30,000 g/mol), LLDPE (Han Yang Chemical, HY3120, melt index = 1.0 g/10 min, density = 0.918 g/cm^3), and MPE (Dow Chemical, DOW 5400, melt index = 1.0 g/10 min, density = 0.916 g/cm^3) are all commercial grade and used without any further treatment.

Sample Compounding

Compounding of PPS/LLDPE and PPS/MPE blends was performed at 290~310 °C by a twin screw compounder (Toshiba, co-rotating intermeshing type, Φ = 35 mm). Tensile and impact specimens were prepared according to ASTM D-638 and D-256 respectively by an Engel ES 240/75P injection molder, and the compositions of PPS/LLDPE and PPS/MPE blends are shown in Table 1.

Rheological Property and Particle Size

Melt viscosity was measured at 300 °C at a shear rate of 10~1000 sec^{-1} by a capillary rheometer (Kayeness Inc., Galaxy III) which consists of a capillary die diameter of 1.5 mm, length of 24.4 mm, and L/D ratio of 16. Particle size of

Table 1. Compositions of PPS/LLDPE and PPS/MPE blends

Entry	1	2	3	4	5	6	7
PPS (wt%)	100	90	80	70	50	30	0
PE (wt%)	0	10	20	30	50	70	100

the blend was measured by (Image Pro Plus for Windows v. 1.2 by Media Cybernetics).

Mechanical Property

Tensile test was done by Lloyd instrument LR 50K (gage length: 100 mm and crosshead speed: 50 mm/min) and an average value from more than five specimens (dogbone type, Type I) made according to ASTM D-638 was used for plotting data. Notched Izod impact strength was measured by an instrument from Testing Machines Inc. (Model 43-02, pendulum 750J, Izod type) and an average data from at least 10 specimens prepared according to ASTM D-256 was used for plotting data, excluding the maximum and minimum values.

Morphological Observation by Electron Microscopy

The fractured surface of PPS/LLDPE and PPS/MPE blends after tensile and notched Izod impact test was given a close look by a JEOL scanning electron microscope (Model JSM-5200) at an operating voltage of 20 kV. The homogeneous dispersion of each component for every blend with different compositions was observed, and the observed morphology was analyzed by Image Pro Plus for Windows (v. 1.3) from Media Cybernetics.

Results and Discussion

Rheological Property

In order to understand particle dispersion of LLDPE and MPE and its impact on structure of PPS/PE blends, rheological property in melt state was investigated. In Figures 1 and 2 which show melt viscosity of PPS/LLDPE or PPS/MPE vs. shear rate change at 300 °C, melt viscosity exponentially decreases with increasing shear rate as generally expected in polymer [10]. This result can be understood from the fact that the convoluted molecular chains of PPS/LLDPE or PPS/MPE start untangling at low shear rate in melt state and disentanglement of polymer chains accelerates with shear rate because the resistance to flow significantly reduces at higher shear rate, immediately reaching the lowest viscosity. The higher melt viscosity than other series of blends was observed for the one with 100 % or 70 % of PE, which suggests that the major presence of PE rather than PPS substantially drags movement of polymeric chains.

In Figure 3, the plots of melt viscosity vs. PE content at two different shear rates (100 and 1000 s^{-1}) are compared, and the melt viscosity of PPS/MPE is slightly higher than that of PPS/LLDPE. At a shear rate of 100 s^{-1}, the melt viscosity of PPS/MPE slowly increased up to 50 wt% of PE, and the similar trend was observed for melt viscosity profile of PPS/LLDPE. The melt viscosity of two blends is sharply contrasted below and above 50 wt% of PE: at more than 50 % of PE a steep increase is observed in comparison with a slow increase rate below 50 wt% of PE.

A slight difference in the melt viscosity of two blends can be understood from the following two points: (1) The MPE prepared by the metallocene catalyst, according to Kaminsky and Brintzinger, has narrower molecular weight distribution

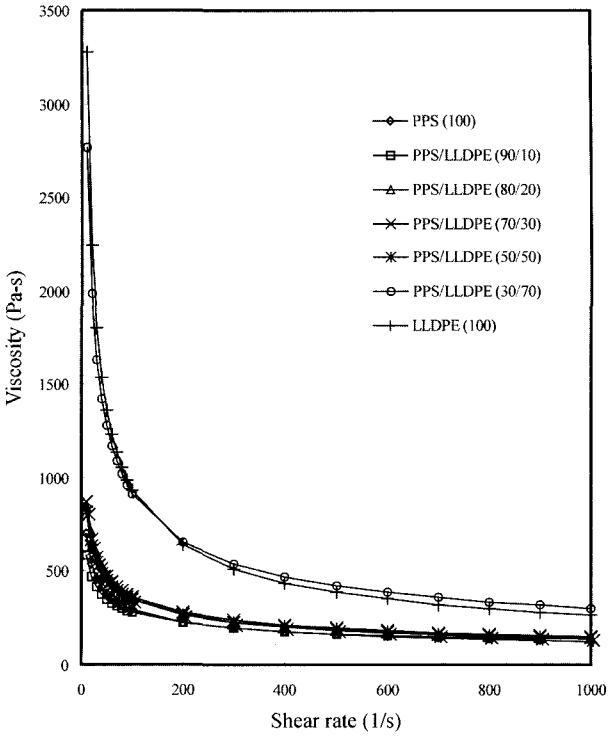

Figure 1. Melt viscosity of PPS/LLDPE blends.

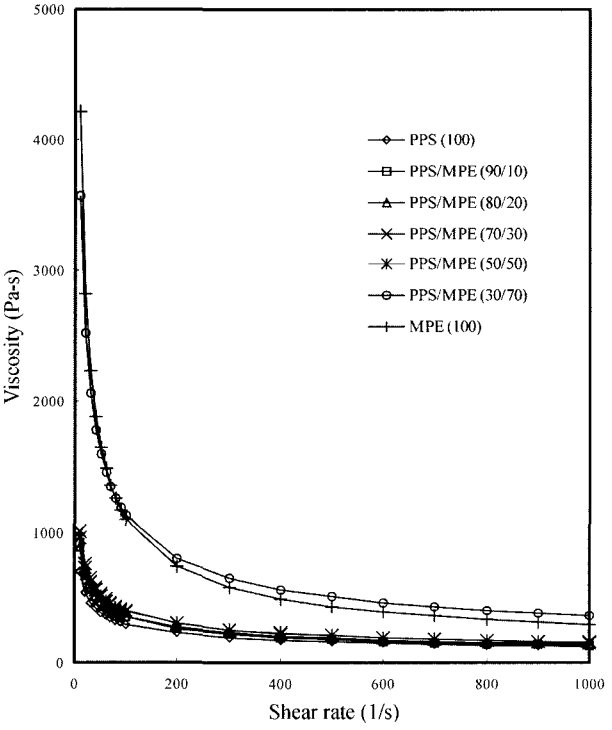

Figure 2. Melt viscosity of PPS/MPE blends.

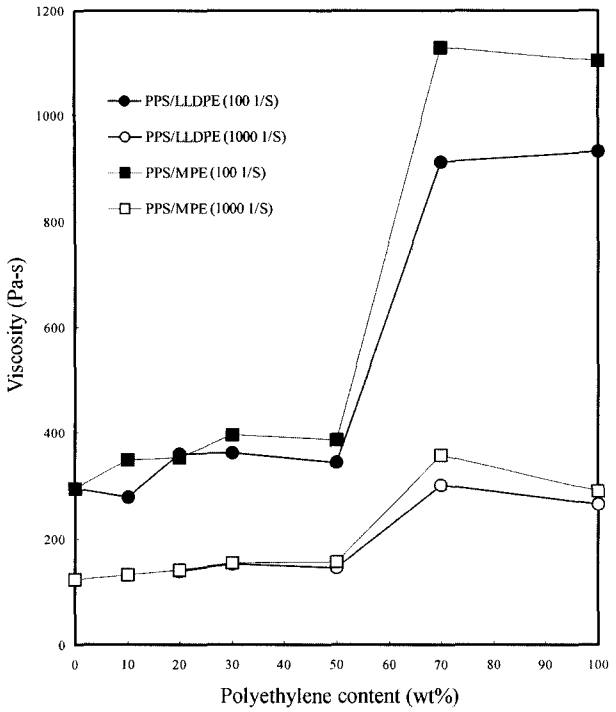

Figure 3. Melt viscosity of PPS/LLDPE and PPS/MPE blends at different shear rate.

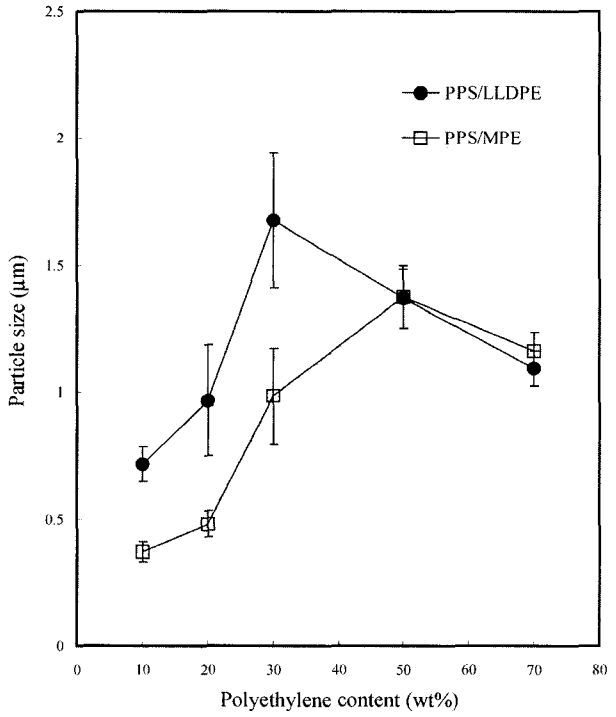

Figure 4. Average dispersed particle size of PPS/LLDPE and PPS/MPE blends (the bar represents 95 % confidence limit).

and more homogeneous comonomer distribution than LLDPE by the Ziegler-Natta catalyst, which results from the constant activity of metallocene catalyst during polymerization, and the resultant difference in degree of plasticization effect can be responsible for the melt viscosity gap; (2) more uniform PE chains of PPS/MPE can evenly penetrate PPS chains during melt mixing process, resulting in higher melt viscosity than that of PPS/LLDPE.

Particle Size and Size Distribution

In Figure 4 showing average particle size of the blends, the particle size increases with the percentage of PE in dispersed state up to 30 wt% and decreases at higher percentage of PE. The largest particle size is observed at 30-40 wt% of PE and PPS/LLDPE has relatively broader size distribution than PPS/MPE. The size distribution increases with particle size for both blends; for example, the size distribution at 30 wt% of PE is about three times greater than that of 10 wt% of PE. From the above results, it seems that PE is not well compatible with PPS at less than 50 wt% of PE and thus results in bulkier particle as more PE is mixed with PPS. Relatively smaller particle size and narrower size distribution of PPS/MPE than those of PPS/LLDPE reflect the compact packing and uniformity of molecular chains of MPE. The decrease of particle size at high PE content originates from effective packing of PE as a major component of blend and insertion of PPS particles into the void space of PE network structure, thus resulting in substantially reduced particle size; such an explanation can be corroborated in the SEM pictures shown in Figure 8(d) and (e). The origin of contrasting properties of PPS and PE can be deduced from the fact that relatively strong attraction among PPS chains by induced dipole-dipole interaction between phenyl rings, and rigid structure of PPS chains containing phenyl rings make PPS very incompatible with PE which has only weak van der Waals interaction among the flexible hydrocarbon chains. The particle size result is in line with the melt viscosity data in showing quite contrasting property at high PE content and such the trend continues in next experimental results.

Tensile Test and Morphological Analysis

In Figure 5 the percent elongations at break of two blends are compared. The elongation at break of PPS/MPE is generally higher than that of PPS/LLDPE and initial peak elongation at break is observed at 10 wt% of PE in dispersed state with immediate decrease at higher PE content. Increase of percent elongation at break at 10 wt% of PE could be coming from the effective tensile energy dispersion via interfacial binding between PPS and PE, and such the result can be related to craze pinning phenomena [2]. Both blends between 20 and 50 wt% of PE have lower percent elongation at break, which is connected with particle size expansion and void space formed inside of the blend. After compounding at a temperature (290~310 °C) higher than T_m of PPS and PE, and molding at the temperature (150 °C) above T_g during injection molding, PPS and dispersed PE sequentially crystallize, and void space

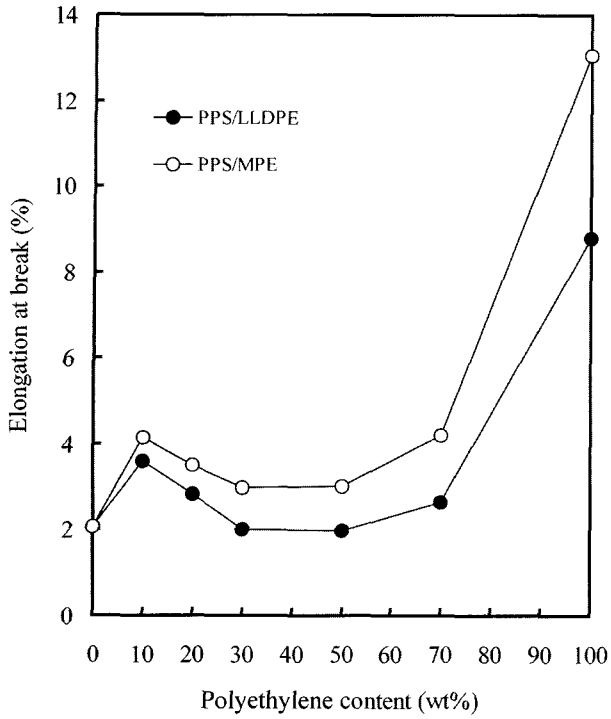

Figure 5. Percent elongation at break vs. polyethylene content of PPS/LLDPE and PPS/MPE blends.

formation accompanies the crystallization. More void space within the blend is formed as more PE is included because PPS has stronger interaction among polymer chains and does not allow void space formation, while PE with its flexible chain and weak inter-chain attraction is forced to house the void space. Particle size expansion with the PE addition in Figure 4 is related to more void space formation and the blend with high void space cannot help but showing low elongation at break. Meanwhile, the surprising increase of percent elongation at break above 50 wt% of PE is due to the flexibility of blend by inclusion of soft PE, and a slightly higher value of MPE suggests more organized and lenient structure of MPE than LLDPE. The rigid structure at low PE percentage and flexible one at high PE content are responsible for the profile and quite different property at high PE content reassures our guess that something interesting is going on inside the blend.

The fractured surfaces of both blends with 10 wt% of PE are compared in Figure 6. For PPS/LLDPE (Figure 6(a)), the surface looks like glass-fractured one, and localized area with plastic deformation, about the size of large particle, can be observed. Some void area on surface indicates the weak interfacial binding between PPS and LLDPE, and the weak structure combined with rigid nature of PPS cannot effectively absorb the external stress. The fractured surface of PPS/MPE at the same PE content also looks brittle, but smaller void space than PPS/LLDPE and less segregation of phase are observed (Figure 6(b)).

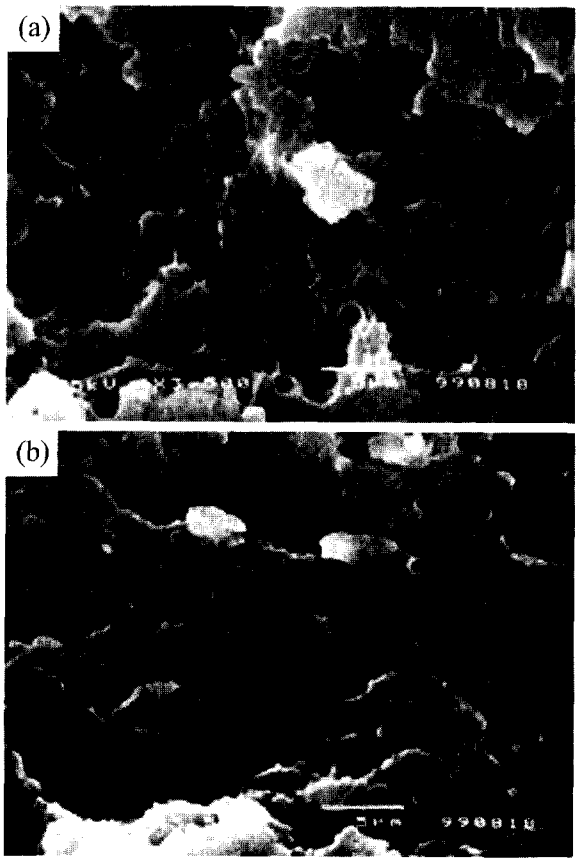

Figure 6. SEM photographs of tensile-fractured surfaces of (a) 90 wt% PPS/10 wt% LLDPE and (b) 90 wt% PPS/10 wt% MPE.

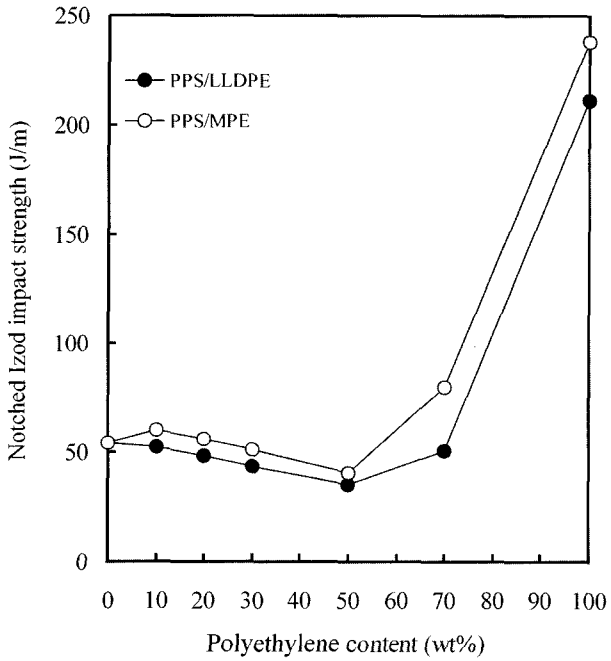

Figure 7. Notched Izod impact strength vs. polyethylene content of PPS/LLDPE and PPS/MPE blends.

Notched Izod Impact Test and Morphological Analysis

Notched Izod impact strength vs. PE content is plotted in Figure 7, showing a similar trend to Figure 5 (plot of elongation at break vs. PE content). The impact strength of two blends decreased little by little as more PE is included up to 50 % and jumped up at PE content higher than 50 %. The steep increase at high PE content could be coming from the effective impact-absorbing ability of the blend as the soft PE becomes a major component at high PE content. The poor impact absorption at low PE content could originate from the fact that PE is not major one any more and the presence of PE as minor component in PPS disrupts the organized structure of PPS. Overall, impact strength of PPS/MPE blends is generally higher than that of PPS/LLDPE blends for entire range of PE, which also tells us that homogeneous polymeric chains of MPE has resulted in well organized structure of PPS/MPE and contributed better than PPS/LLDPE in absorbing external impact.

Figure 8 shows the surfaces of impact-fractured PPS, PPS/LLDPE, and PPS/MPE. The PPS by itself looks brittle and has a typical fractured surface (Figure 8(a)). The PPS/LLDPE one with 10 wt% of PE also shows brittle surface, suggesting that PPS still dominates overall surface structure of the blend and addition of PE as a minor component does not help much in modifying the surface structure (Figure 8(b)). Not much difference is found in the fractured surface of PPS/MPE with 10 wt% of PE as compared to Figure 8(b), because PPS is again the major component of blend and the small difference in PE molecular chains does not radically change the apparent shape of blend (Figure 8(c)). In Figure 8(d) and

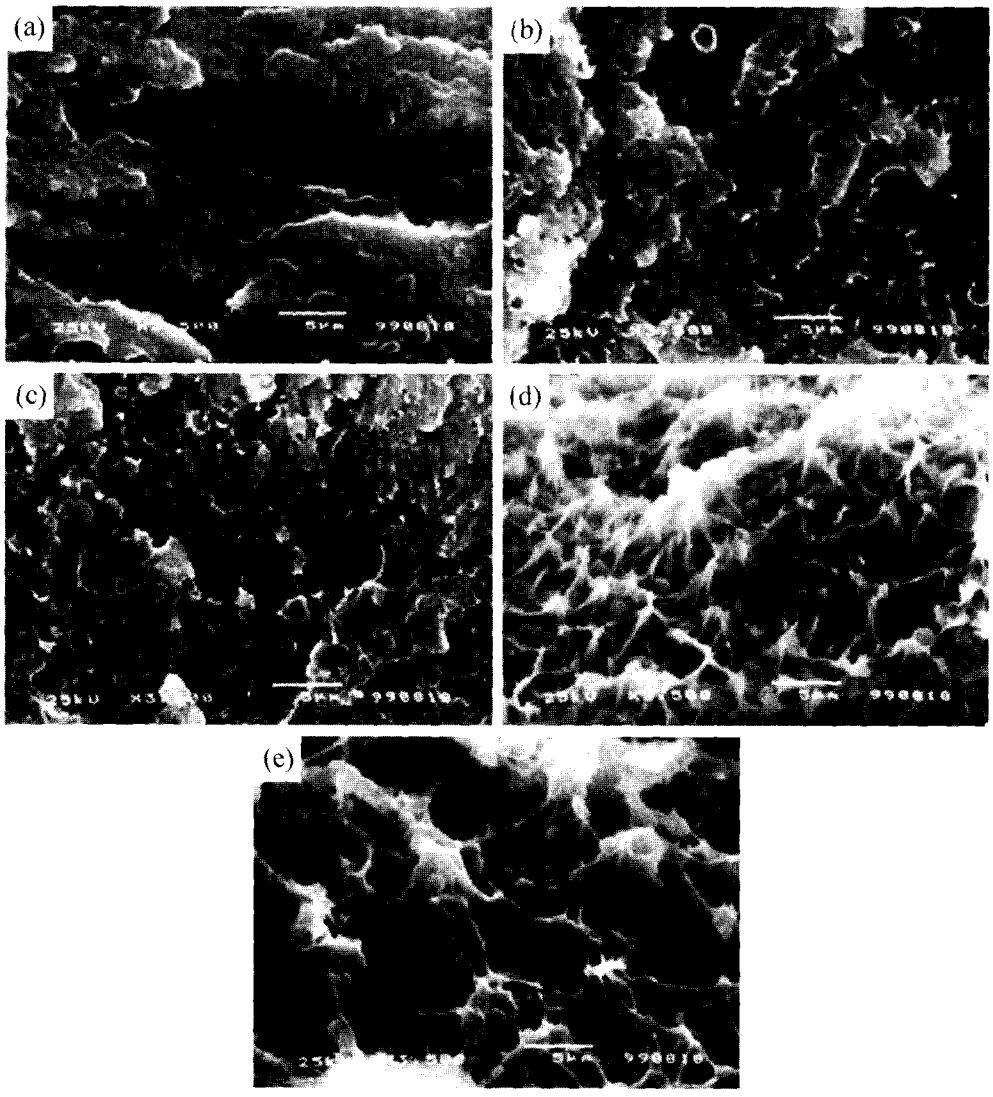

Figure 8. SEM photographs of impact-fractured surfaces of (a) pure PPS, (b) 90 wt% PPS/10 wt% LLDPE, (c) 90 wt% PPS/10 wt% MPE, (d) 30 wt% PPS/70 wt% LLDPE, and (e) 30 wt% PPS/70 wt% MPE.

(e), in which the composition has reversed, PE now fills up most of the surface and PPS shows its presence as small particles. Based on the surface morphology by SEM, it seems that nice combination of network structure of PE and filling-up of PPS particle in the hole of PE network enables achieving effective external impact absorption and thus answers the reason why mechanical properties have substantially increased at high PE percentages. The difference between Figure 8(d) and (e) is not clear yet and the minor difference in PE structure cannot be dissected as in the case of Figure 8(b) and (c). The search for finding better PPS blends continues in our laboratory.

Conclusion

Two PEs (LLDPE or MPE) were melt-blended with PPS and the blends were investigated in the points of rheological and mechanical properties. PPS/PE blend shows better properties than PPS/LLDPE in overall results and the substantial increase of the properties was observed at 70 % PE content as supported in SEM pictures. Particle size expansion and void area formation seem to be correlated in 20-50 wt% PE region, and the blends at that ratio are not recommended for practical application due to its poor mechanical performance. In conclusion, we have investigated and found a good ratio of PPS/PE blend for improving impact absorption of PPS, and further fine-tuning of the blend with other type of polymer remains to be finished.

Acknowledgement

The specimen preparation by SK Chemical Co. is greatly appreciated.

References

1. T. H. Chen and A. C. Su, *Polymer*, **34**, 4826 (1993).
2. S. I. Lee and B. C. Chun, *Polymer*, **39**, 6441 (1998).
3. J. Masamoto and K. Kubo, *Polym. Eng. Sci.*, **36**, 256 (1996).
4. J. H. Choi and S. H. Lim, *Polymer*, **38**, 4401 (1997).
5. G. P. Desio and L. J. Rebenfeld, *J. Appl. Polym. Sci.*, **44**, 1989 (1992).
6. S. S. Song, J. L. White, and M. Cakmak, *Polym. Eng. Sci.*, **30**, 944 (1990).
7. V. L. Shingankuli, J. P. Jog, and M. J. Nadkarini, *J. Appl. Polym. Sci.*, **36**, 335 (1988).
8. L. Rebenfeld, G. P. Desio, and J. C. Wu, *J. Appl. Polym. Sci.*, **42**, 801 (1991).
9. J. S. Chung and P. Cebe, *Polymer*, **33**, 2312 (1992).
10. S. Balakrishnan, N. R. Neelakantan, D. N. Saheb, and J. P. Jog, *Polymer*, **39**, 5765 (1998).
11. A. Maffezzoli, J. M. Kenny, and L. Nicolais, *Thermochimica Acta*, **199**, 133 (1992).
12. L. I. Minkova and P. L. Magagnini, *Polym. Eng. Sci.*, **32**, 57 (1992).